Correlating $A \to \gamma\gamma$ with electric dipole moments in the two Higgs doublet model in light of the diphoton excesses at 95 GeV and 152 GeV

Sumit Banik,[1,2,*] Guglielmo Coloretti,[1,2,†] Andreas Crivellin,[1,2,‡] and Howard E. Haber[3,§]

[1]*Physik-Institut, Universität Zürich, Winterthurerstrasse 190, CH–8057 Zürich, Switzerland*
[2]*Laboratory for Particle Physics, PSI Center for Neutron and Muon Sciences, Forschungsstrasse 111, 5232 Villigen PSI, Switzerland*
[3]*Santa Cruz Institute for Particle Physics, University of California, 1156 High Street, Santa Cruz, California 95064, USA*

(Received 9 December 2024; accepted 13 March 2025; published 15 April 2025)

We examine the correlations between new scalar boson decays to photons and electric dipole moments (EDMs) in the CP-violating flavor-aligned two-Higgs-doublet model (2HDM). It is convenient to work in the Higgs basis $\{\mathcal{H}_1, \mathcal{H}_2\}$ where only the first Higgs doublet field $\mathcal{H}_1$ acquires a vacuum expectation value. In light of the LHC Higgs data, which agree well with Standard Model (SM) predictions, it follows that the parameters of the 2HDM are consistent with the Higgs alignment limit. In this parameter regime, the observed SM-like Higgs boson resides almost entirely in $\mathcal{H}_1$, and the other two physical neutral scalars, which reside almost entirely in $\mathcal{H}_2$, are approximate eigenstates of CP (denoted by the CP-even H and the CP-odd A). In the Higgs basis, the scalar potential term $\bar{Z}_7\mathcal{H}_1^\dagger\mathcal{H}_2\mathcal{H}_2^\dagger\mathcal{H}_2 + \text{H.c.}$ governs the charged-Higgs loop contributions to the decay of H and A to photons. If $\operatorname{Re}\bar{Z}_7 \operatorname{Im}\bar{Z}_7 \neq 0$, then CP-violating effects are present and allow for an H^+H^-A coupling, which can yield a sizable branching ratio for $A \to \gamma\gamma$. These CP-violating effects also generate nonzero EDMs for the electron, the neutron and the proton. We examine these correlations for the cases of $m_A = 95$ GeV and $m_A = 152$ GeV where interesting excesses in the diphoton spectrum have been observed at the LHC. These excesses can be explained via the decay of A while being consistent with the experimental bound for the electron EDM in regions of parameter space that can be tested with future neutron and proton EDM measurements. This allows for the interesting possibility where the 95 GeV diphoton excess can be identified with A, while $m_H \simeq 98$ GeV can account for the best fit to the LEP excess in $e^+e^- \to ZH$ with $H \to b\bar{b}$.

DOI: 10.1103/PhysRevD.111.075021

I. INTRODUCTION

With the discovery of the Higgs boson at the Large Hadron Collider (LHC) [1,2], the Standard Model (SM) of particle physics is complete. Furthermore, the SM has been remarkably successful in describing the interactions of fundamental particles and their interactions (although there are a number of anomalies that, if verified in subsequent experimental studies, could provide definitive evidence for a breakdown of the SM [3]).

Nevertheless, there is some motivation to extend the SM by adding additional scalar multiplets, as there is no consistency principle that requires the minimal realization of the Higgs sector in which one complex Higgs doublet with hypercharge $Y = \frac{1}{2}$ generates mass for the $W^\pm$ and Z gauge bosons, the quarks, and the charged leptons. Indeed, in light of the observation that the SM possesses three generations of quarks and leptons, one might also expect additional generations of scalars (e.g., see Refs. [4–10]). Another indication of the need for additional scalars arises when attempting to devise a theory of electroweak baryogenesis to explain the observed asymmetry between baryons and antibaryons (e.g., see Ref. [11]), which cannot be achieved by the SM alone.

One of the most well-studied extensions of the SM scalar sector, which is obtained by adding a second complex Higgs doublet with hypercharge $Y = \frac{1}{2}$, is the two-Higgs-doublet

*Contact author: sumit.banik@psi.ch
†Contact author: guglielmo.coloretti@physik.uzh.ch
‡Contact author: andreas.crivellin@cern.ch
§Contact author: haber@scipp.ucsc.edu

model (2HDM) [4] (see Ref. [12] for a comprehensive review). The 2HDM provides opportunities for addressing the issues mentioned above while remaining compatible with electroweak precision data.

In its most general form, the 2HDM possesses new sources of CP violation due to additional complex parameters in the Higgs Lagrangian. Such models can be compatible with a strong first-order electroweak phase transition needed for generating a sufficient baryon asymmetry in the early Universe [13–19]. However, in specialized versions of the 2HDM with natural flavor conservation, usually implemented via a $\mathbb{Z}_2$ symmetry [20–22], there is only one additional physical complex phase in the scalar potential, such that achieving a large enough baryon asymmetry is challenging [23]. This difficulty can be overcome by giving up the $\mathbb{Z}_2$ symmetry and considering a more general 2HDM with additional sources of CP violation.

However, new complex phases also give rise to contributions to low-energy probes of CP violation, in particular, electric dipole moments (EDMs) [24–26]. In the general CP-violating 2HDM, the EDM of the electron typically places the most stringent bound on the model parameters [27–29]. In some cases, future neutron and proton EDM measurements also have the potential to constrain the CP-violating parameters of the model.

In the 2HDM with a SM-like Higgs boson (as required in light of LHC Higgs data [30,31]), there are two additional neutral scalars that are often approximate eigenstates of CP, denoted by the CP-even H and the CP-odd A. Sizable branching ratios of H and A decays into photons are phenomenologically motivated by the $\gamma\gamma$ excesses at 95 GeV [32–35] and 152 GeV [36–44].[1] In particular, it has been shown that it is difficult to achieve the rates preferred by data, especially if the CP-odd state is responsible for the excess at 95 GeV or 152 GeV within different versions of the 2HDM (see Refs. [49–52] and [53], respectively). In this paper, our aim is to broaden the treatment of the 2HDM version employed in analyzing these excesses, paying close attention to the correlations of the decay rate of $A \to \gamma\gamma$ with the EDMs of the electron, neutron, and proton.

In Sec. II, we review the most general CP-violating 2HDM, using the basis independent formalism introduced in Refs. [54–57]. In Sec. III, the decay widths of the neutral Higgs bosons to two photons are obtained for the most general CP-violating 2HDM, and in Sec. IV, the electron, neutron and proton EDMs are considered. In light of the EDM constraints, the viability of the general CP-violating 2HDM to explain the excesses in the $\gamma\gamma$ channel at 95 GeV or 152 GeV is examined in Sec. V, under the assumption that one of the two experimental excesses represents new physics beyond the SM. Brief conclusions are presented in Sec. VI, followed by two appendices that provide details on the 2HDM Yukawa sector and summarize the loop functions employed in calculating the diphoton decays of the neutral scalars.

II. 2HDM FORMALISM

The 2HDM employs two complex $\mathrm{SU}(2)_L$ doublets scalars Φ_1 and Φ_2 with hypercharge $Y = \frac{1}{2}$. In the most general version of the 2HDM, the fields Φ_1 and Φ_2 are indistinguishable. Thus, it is always possible to define a new basis of scalar fields, $\Phi'_i = \sum_{j=1}^{2} U_{ij}\Phi_j$ for $i = 1, 2$, where U is a 2×2 unitary matrix. In particular, one can always transform from the scalar field basis $\{\Phi_1, \Phi_2\}$ to the Higgs basis [54,58–62], denoted by $\{\mathcal{H}_1, \mathcal{H}_2\}$, such that $\langle \mathcal{H}_1^0 \rangle = v/\sqrt{2}$ and $\langle \mathcal{H}_2^0 \rangle = 0$, with $v \equiv (\sqrt{2}G_F)^{-1/2} \simeq 246$ GeV, where G_F is the Fermi constant. Requiring renormalizability and $\mathrm{SU}(2)_L \times U(1)_Y$ gauge invariance, the most general scalar potential in the Higgs basis is given by

$$\begin{aligned}\mathcal{V} = {} & Y_1 \mathcal{H}_1^\dagger \mathcal{H}_1 + Y_2 \mathcal{H}_2^\dagger \mathcal{H}_2 + [Y_3 e^{-i\eta} \mathcal{H}_1^\dagger \mathcal{H}_2 + \text{H.c.}] + \frac{1}{2} Z_1 (\mathcal{H}_1^\dagger \mathcal{H}_1)^2 + \frac{1}{2} Z_2 (\mathcal{H}_2^\dagger \mathcal{H}_2)^2 + Z_3 (\mathcal{H}_1^\dagger \mathcal{H}_1)(\mathcal{H}_2^\dagger \mathcal{H}_2) \\ & + Z_4 (\mathcal{H}_1^\dagger \mathcal{H}_2)(\mathcal{H}_2^\dagger \mathcal{H}_1) + \left\{ \frac{1}{2} Z_5 e^{-2i\eta} (\mathcal{H}_1^\dagger \mathcal{H}_2)^2 + [Z_6 e^{-i\eta} \mathcal{H}_1^\dagger \mathcal{H}_1 + Z_7 e^{-i\eta} \mathcal{H}_2^\dagger \mathcal{H}_2] \mathcal{H}_1^\dagger \mathcal{H}_2 + \text{H.c.} \right\},\end{aligned} \tag{1}$$

where Y_1, Y_2, and $Z_1, \ldots, Z_4$ are real, whereas Y_3, Z_5, Z_6, and Z_7 are (potentially) complex parameters. The minimization of the Higgs basis scalar potential yields

$$Y_1 = -\frac{1}{2} Z_1 v^2, \qquad Y_3 = -\frac{1}{2} Z_6 v^2. \tag{2}$$

The presence of the complex phase $e^{-i\eta}$ in Eq. (1) accounts for the nonuniqueness of the Higgs basis, since one is always free to rephase $\mathcal{H}_2$ because its vacuum expectation value vanishes. In particular, under a U(2) basis transformation $\Phi_i \to U_{ij}\Phi_j$, the Higgs basis fields $\mathcal{H}_1$ and $\mathcal{H}_2$ are *invariant*

[1] The existence of a boson of mass $\sim$150 GeV was first proposed in the context of the multilepton anomalies (see Refs. [3,45] for reviews) in WW final states [46], later found to be compatible with transverse mass [47] differential top-quark distributions [48].

whereas the phase factor $e^{-i\eta}$ transforms as $e^{-i\eta} \to (\det U) e^{-i\eta}$, where $\det U \equiv e^{i\phi}$ (such that $\phi \in \mathbb{R}$) is a complex number of unit modulus. It follows that the quantities Y_1, Y_2, and $Z_1, \ldots, Z_4$ are invariant with respect to a change of basis of the scalar fields, whereas $[Y_3, Z_6, Z_7] \to e^{-i\phi}[Y_3, Z_6, Z_7]$ and $Z_5 \to e^{-2i\phi} Z_5$. Therefore,

$$\bar{Z}_5 \equiv Z_5 e^{-2i\eta}, \qquad \bar{Z}_6 \equiv Z_6 e^{-i\eta}, \qquad \bar{Z}_7 \equiv Z_7 e^{-i\eta}, \tag{3}$$

are basis-invariant quantities.[2]

In the Higgs basis the scalar doublets can be parametrized as

$$\mathcal{H}_1 = \begin{pmatrix} G^+ \\ \frac{1}{\sqrt{2}}(v + \varphi_1^0 + iG) \end{pmatrix}, \qquad \mathcal{H}_2 = \begin{pmatrix} \mathcal{H}_2^+ \\ \frac{1}{\sqrt{2}}(\varphi_2^0 + ia^0) \end{pmatrix}, \tag{4}$$

where we have identified $G = \sqrt{2}\,\mathrm{Im}\,\mathcal{H}_1^0$ and $G^\pm = \mathcal{H}_1^\pm$ as the massless CP-odd neutral and charged Goldstone bosons, respectively, and $\mathcal{H}_2^\pm$ as the physical charged Higgs boson pair with

$$m_{H^\pm}^2 = Y_2 + \frac{1}{2} Z_3 v^2. \tag{5}$$

In general, the CP-even scalar φ_1^0 mixes with the scalars φ_2^0 and a^0.

The resulting physical neutral scalar squared-mass matrix in the φ_1^0–φ_2^0–a^0 basis is

$$\mathcal{M}^2 = v^2 \begin{pmatrix} Z_1 & \mathrm{Re}\,\bar{Z}_6 & -\mathrm{Im}\,\bar{Z}_6 \\ \mathrm{Re}\,\bar{Z}_6 & \frac{1}{2}[Z_{4c} + \mathrm{Re}\,\bar{Z}_5] & -\frac{1}{2}\mathrm{Im}\,\bar{Z}_5 \\ -\mathrm{Im}\,\bar{Z}_6 & -\frac{1}{2}\mathrm{Im}\,\bar{Z}_5 & \frac{1}{2}[Z_{4c} - \mathrm{Re}\,\bar{Z}_5] \end{pmatrix}, \tag{6}$$

where $Z_{4c} \equiv Z_4 + 2m_{H^\pm}^2/v^2$, and the quantities $\bar{Z}_5$ and $\bar{Z}_6$ are defined in Eq. (3). If $\mathrm{Im}\,\bar{Z}_5 = \mathrm{Im}(\bar{Z}_6)^2 = 0$ then there is no mixing of the would-be CP-even and CP-odd neutral scalar states in the neutral scalar squared-mass matrix. If these conditions do not hold, then CP-violating interactions of the neutral scalar mass eigenstates are present.[3]

Since the squared-mass matrix $\mathcal{M}^2$ is real and symmetric, it can be diagonalized by an orthogonal transformation with unit determinant,

$$R\mathcal{M}^2 R^\mathsf{T} = \mathcal{M}_D^2 \equiv \mathrm{diag}(m_1^2, m_2^2, m_3^2), \tag{7}$$

where $RR^\mathsf{T} = I$, $\det R = 1$, and the m_k^2 are the eigenvalues of $\mathcal{M}^2$. A convenient form for R is

$$R = \begin{pmatrix} c_{13}c_{12} & -s_{12}c_{23} - c_{12}s_{13}s_{23} & -c_{12}s_{13}c_{23} + s_{12}s_{23} \\ c_{13}s_{12} & c_{12}c_{23} - s_{12}s_{13}s_{23} & -s_{12}s_{13}c_{23} - c_{12}s_{23} \\ s_{13} & c_{13}s_{23} & c_{13}c_{23} \end{pmatrix}, \tag{8}$$

where $c_{ij} \equiv \cos\theta_{ij}$ and $s_{ij} \equiv \sin\theta_{ij}$. Indeed, the angles θ_{12}, θ_{13}, and θ_{23} defined above are basis-invariant quantities since they are obtained by diagonalizing $\mathcal{M}^2$, whose matrix elements are independent of the choice of the scalar field basis.

The neutral physical scalar mass eigenstates, denoted by h_1, h_2, and h_3 (with corresponding masses m_1, m_2, and m_3), are given by

$$\begin{pmatrix} h_1 \\ h_2 \\ h_3 \end{pmatrix} = R \begin{pmatrix} \varphi_1^0 \\ \varphi_2^0 \\ a^0 \end{pmatrix} = Q \begin{pmatrix} \sqrt{2}\,\mathrm{Re}\,\mathcal{H}_1^0 - v \\ \mathcal{H}_2^0 \\ \mathcal{H}_2^{0\dagger} \end{pmatrix}, \tag{9}$$

where

$$Q = \begin{pmatrix} q_{11} & \frac{1}{\sqrt{2}} q_{12}^* e^{i\theta_{23}} & \frac{1}{\sqrt{2}} q_{12} e^{-i\theta_{23}} \\ q_{21} & \frac{1}{\sqrt{2}} q_{22}^* e^{i\theta_{23}} & \frac{1}{\sqrt{2}} q_{22} e^{-i\theta_{23}} \\ q_{31} & \frac{1}{\sqrt{2}} q_{32}^* e^{i\theta_{23}} & \frac{1}{\sqrt{2}} q_{32} e^{-i\theta_{23}} \end{pmatrix}, \tag{10}$$

and the q_{kj} are defined in Table I.

It is convenient to define the positively charged Higgs field as

$$H^+ \equiv e^{i\theta_{23}} \mathcal{H}_2^+. \tag{11}$$

One can then invert Eq. (9) and include the charged scalars to obtain

$$\mathcal{H}_1 = \begin{pmatrix} G^+ \\ \frac{1}{\sqrt{2}}\left(v + iG + \sum_{k=1}^3 q_{k1} h_k\right) \end{pmatrix} \tag{12}$$

and

TABLE I. The basis-invariant quantities $q_{k\ell}$ are functions of the neutral scalar mixing angles θ_{12} and θ_{13}, with $c_{ij} \equiv \cos\theta_{ij}$ and $s_{ij} \equiv \sin\theta_{ij}$. The angles θ_{12}, θ_{23} are defined modulo π. By convention, we take $0 \le c_{12}, c_{13} \le 1$.

k	q_{k1}	q_{k2}
1	$c_{12}c_{13}$	$-s_{12} - ic_{12}s_{13}$
2	$s_{12}c_{13}$	$c_{12} - is_{12}s_{13}$
3	s_{13}	ic_{13}

[2]Note that physical observables can depend only on basis-invariant combinations of the scalar potential parameters.

[3]Another potential source of CP violation in the scalar self-interactions is due to the complex parameter $\bar{Z}_7$, which does not appear in the mass matrix in Eq. (6) and is thus uncorrelated with the mixing among the neutral scalars.

$$e^{i\theta_{23}}\mathcal{H}_2 = \begin{pmatrix} H^+ \\ \frac{1}{\sqrt{2}}\sum_{k=1}^3 q_{k2}h_k \end{pmatrix}. \tag{13}$$

Although θ_{23} is a basis invariant parameter, it has no physical significance since it can be eliminated by rephasing the scalar doublet field $\mathcal{H}_2 \to e^{-i\theta_{23}}\mathcal{H}_2$. Henceforth, we shall set $\theta_{23} = 0$ as advocated in Refs. [63,64].

To perform a phenomenological analysis, it is instructive to identify a set of independent basis-invariant parameters that govern the scalar sector of the most general 2HDM. First, we rewrite Eq. (7) as $\mathcal{M}^2 = R^\mathsf{T}\mathcal{M}_D^2 R$ and insert the expression for R given by Eq. (8) with $\theta_{23} = 0$. We then make use of Eq. (6) to obtain

$$Z_1 = \frac{1}{v^2}\sum_{k=1}^3 m_k^2 (q_{k1})^2, \tag{14}$$

$$Z_4 = \frac{1}{v^2}\left[\sum_{k=1}^3 m_k^2 |q_{k2}|^2 - 2m_{H^\pm}^2\right], \tag{15}$$

$$\bar{Z}_5 = \frac{1}{v^2}\sum_{k=1}^3 m_k^2 (q_{k2}^*)^2, \tag{16}$$

$$\bar{Z}_6 = \frac{1}{v^2}\sum_{k=1}^3 m_k^2 q_{k1} q_{k2}^*. \tag{17}$$

Together with Eqs. (2) and (5) it follows that a convenient choice for the set of independent parameters is

$$\{v, \theta_{12}, \theta_{13}, m_1, m_2, m_3, m_{H^\pm}, Z_2, Z_3, \mathrm{Re}\,\bar{Z}_7, \mathrm{Im}\,\bar{Z}_7\}, \tag{18}$$

where the complex parameter $\bar{Z}_7$ is defined in Eq. (3). That is, the scalar sector of the most general 2HDM is governed by 11 real independent basis-invariant parameters.

The LHC Higgs data strongly suggest that the observed Higgs scalar of mass 125 GeV is SM-like [30,31]. We shall identify this scalar with $h_1 \simeq h_{\rm SM}$. As the $W^+W^-h_k$ terms in the Lagrangian are given by

$$W_\mu^+ W_\nu^- h_k: \qquad g m_W q_{k1} g_{\mu\nu}, \tag{19}$$

for $k = 1, 2, 3$, it follows that the $h_1 W^+W^-$ coupling coincides with that of the SM Higgs boson if $q_{11} = 1$, which corresponds to the Higgs alignment limit [65–70]. In this limit, $c_{12} = c_{13} = 1$ and $s_{12} = s_{13} = 0$ (or equivalently, $q_{11} = q_{22} = -iq_{32} = 1$ and $q_{21} = q_{31} = q_{12} = 0$ in light of Table I). Using Eqs. (16) and (17), one obtains

$$\mathrm{Im}\,\bar{Z}_5 = \bar{Z}_6 = 0, \qquad (\text{Higgs alignment limit}). \tag{20}$$

The conditions for a CP-conserving scalar sector are given by [54]:

$$\mathrm{Im}(\bar{Z}_5^*\bar{Z}_6^2) = \mathrm{Im}(\bar{Z}_5^*\bar{Z}_7^2) = \mathrm{Im}(\bar{Z}_6^*\bar{Z}_7) = 0. \tag{21}$$

Whereas $\bar{Z}_7$ does not appear in the neutral scalar squared-mass matrix, it provides a potentially new source of CP-violation via the scalar self-interactions. For example, the $H^+H^-h_k$ terms that appear in the scalar Lagrangian, obtained after inserting Eqs. (12) and (13) into Eq. (1), are given by

$$H^+H^-h_k: \qquad -v[q_{k1}Z_3 + \mathrm{Re}(q_{k2}\bar{Z}_7)], \tag{22}$$

with $k = 1, 2, 3$. These interactions are relevant for the charged Higgs boson loop contribution to the $h_k \to \gamma\gamma$ decay amplitude because they give unsuppressed contributions in the Higgs alignment limit. Therefore we have used them in Sec. III to generate a sizable branching ratio of h_2 and h_3 to two photons.

As a result of Eqs. (20) and (21), it follows that the scalar sector is CP-conserving if and only if,

$$\mathrm{Im}(\bar{Z}_5^*\bar{Z}_7^2) = 2\bar{Z}_5\,\mathrm{Re}\,\bar{Z}_7\,\mathrm{Im}\,\bar{Z}_7 = 0. \tag{23}$$

Under the assumption of $m_2 \neq m_3$, $\bar{Z}_5$ is real and nonzero [see Eq. (16)], in which case CP conservation requires that either $\mathrm{Re}\,\bar{Z}_7 = 0$ or $\mathrm{Im}\,\bar{Z}_7 = 0$. In the Higgs alignment limit, the $H^+H^-h_k$ couplings are given by

$$H^+H^-h_1: \qquad -vZ_3, \tag{24}$$

$$H^+H^-h_2: \qquad -v\,\mathrm{Re}\,\bar{Z}_7, \tag{25}$$

$$H^+H^-h_3: \qquad v\,\mathrm{Im}\,\bar{Z}_7. \tag{26}$$

Since H^+H^- is CP-even, it follows that h_1 is CP-even in the Higgs alignment limit, whereas h_2 is CP-even and h_3 is CP-odd if $\mathrm{Im}\,\bar{Z}_7 = 0$.[4] In contrast, if $\mathrm{Re}\,\bar{Z}_7\,\mathrm{Im}\,\bar{Z}_7 \neq 0$, then h_2 and h_3 are states of indefinite CP and the scalar sector is CP-violating.

In practice the Higgs alignment limit of the 2HDM is not exact. Indeed, the LHC Higgs data (which confirms that h_1 is SM-like) only requires that $|s_{12}|$, $|s_{13}| \ll 1$. Consider the case of $0 < |s_{12}| \ll 1$ and $s_{13} = 0$. Then Eqs. (16) and (17) yield $\mathrm{Im}\,\bar{Z}_5 = \mathrm{Im}\,\bar{Z}_6 = 0$. If in addition $\bar{Z}_7 = 0$, then the bosonic sector is CP-conserving and we can identify $h_2 \equiv H$ and $h_3 \equiv A$, where we have employed the standard notation of the 2HDM where H is CP-even and A is CP-odd. It is then

[4]Note that if $\mathrm{Re}\,\bar{Z}_7 = 0$ then h_2 is CP-odd and h_3 is CP-even in the Higgs alignment limit. That is, the CP properties of h_2 and h_3 are reversed with respect to the case of $\mathrm{Im}\,\bar{Z}_7 = 0$. If $\bar{Z}_7 = 0$, then the CP quantum numbers of h_2 and h_3 are not individually determined even though the bosonic sector of the theory is CP-conserving and the presence of the Zh_2h_3 coupling indicates that the product of fields h_2h_3 is CP-odd.

useful to maintain the H, A notation even when $\bar{Z}_7 \neq 0$, in which case, an H^+H^-A coupling (which violates CP) will be present if $\mathrm{Im}\,\bar{Z}_7 \neq 0$ as indicated in Eq. (26). Similarly, if $0 < |s_{13}| \ll 1$ and $s_{12} = 0$, then it follows that $\mathrm{Im}\,\bar{Z}_5 = \mathrm{Re}\,\bar{Z}_6 = 0$, in which case we can identify $h_2 \equiv A$ and $h_3 \equiv H$. In this scenario, an H^+H^-A coupling (which violates CP) will be present if $\mathrm{Re}\,\bar{Z}_7 \neq 0$ as indicated in Eq. (25).

Finally, we examine the Higgs-fermion couplings of the 2HDM. In the absence of a $\mathbb{Z}_2$ symmetry to constrain the Higgs Lagrangian, both scalar doublets will couple to up-type and down-type fermions in the Yukawa Lagrangian,

$$-\mathcal{L}_Y = \bar{Q}(\hat{\boldsymbol{\kappa}}_{\boldsymbol{U}}\tilde{\mathcal{H}}_1 + \hat{\boldsymbol{\rho}}_{\boldsymbol{U}}\tilde{\mathcal{H}}_2)U + \bar{Q}(\hat{\boldsymbol{\kappa}}_{\boldsymbol{D}}^\dagger\mathcal{H}_1 + \hat{\boldsymbol{\rho}}_{\boldsymbol{D}}^\dagger\mathcal{H}_2)D + \bar{L}(\hat{\boldsymbol{\kappa}}_{\boldsymbol{E}}^\dagger\mathcal{H}_1 + \hat{\boldsymbol{\rho}}_{\boldsymbol{E}}^\dagger\mathcal{H}_2)E + \text{H.c.}, \qquad (27)$$

where $\bar{Q}\tilde{\mathcal{H}}_k \equiv \bar{Q}^1\mathcal{H}_k^{2\dagger} - \bar{Q}^2\mathcal{H}_k^{1\dagger}$, $\bar{Q}\mathcal{H}_k \equiv \bar{Q}^i\mathcal{H}_k^i$, and $\bar{L}\mathcal{H}_k \equiv \bar{L}^i\mathcal{H}_k^i$, summed over the repeated $\mathrm{SU}(2)_L$ superscript index i, for $k = 1, 2$. In Eq. (27), $\hat{\boldsymbol{\kappa}}_{\boldsymbol{F}}$, $\hat{\boldsymbol{\rho}}_{\boldsymbol{F}}$ (for $F = U, D, E$) are 3×3 Yukawa coupling matrices, Q and L are $\mathrm{SU}(2)_L$ doublets of left-handed quark and lepton fields, and U, D and E are $\mathrm{SU}(2)_L$ singlets of right-handed quark and lepton fields (with the generation index suppressed). When the fermion mass matrices, $\hat{\boldsymbol{M}}_{\boldsymbol{F}} \equiv v\hat{\boldsymbol{\kappa}}_{\boldsymbol{F}}/\sqrt{2}$, are diagonalized, the corresponding transformed $\hat{\boldsymbol{\rho}}_{\boldsymbol{F}}$ matrices are in general complex and nondiagonal. That is, without further restrictions on the Yukawa Lagrangian, natural flavor conservation cannot be enforced [71,72]. As a result, the most general 2HDM will generically yield dangerously large flavor-changing neutral currents at tree-level mediated by neutral scalars (e.g., see Ref. [73] for a detailed analysis).

An alternative approach to avoid off-diagonal neutral scalar couplings to fermions is to impose alignment in flavor space on the Yukawa couplings of the two scalar doublets [64,74–80]. That is, we define (potentially complex) flavor alignment parameters a_F in Eq. (27) via[5]:

$$\hat{\boldsymbol{\rho}}_{\boldsymbol{F}} = \frac{\sqrt{2}}{v}a_F\hat{\boldsymbol{M}}_{\boldsymbol{F}}, \quad \text{for } F = U, D, E. \qquad (28)$$

Note that the Yukawa coupling matrices defined in Eq. (27) and the flavor alignment parameters a_F are invariant with respect to a change of basis of the scalar fields.

In Appendix A, we obtain the Yukawa Lagrangian involving the neutral scalar fields h_k [cf. Eq. (A11)]:

$$-\mathcal{L}_Y = \frac{1}{v}\bar{U}\boldsymbol{M}_{\boldsymbol{U}}\sum_{k=1}^{3}(q_{k1} + q_{k2}^* a_U\mathcal{P}_R + q_{k2}a_U^*\mathcal{P}_L)Uh_k + \frac{1}{v}\sum_{F=D,E}\bar{F}\boldsymbol{M}_{\boldsymbol{F}}\sum_{k=1}^{3}(q_{k1} + q_{k2}a_F^*\mathcal{P}_R + q_{k2}^* a_F\mathcal{P}_L)Fh_k. \qquad (29)$$

In the exact Higgs alignment limit, Eq. (29) reduces to

$$-\mathcal{L}_Y = \frac{1}{v}\sum_{F=U,D,E}\bar{F}\boldsymbol{M}_{\boldsymbol{F}}Fh_1 + \frac{1}{v}\sum_{F=U,D,E}\bar{F}\boldsymbol{M}_{\boldsymbol{F}}(\mathrm{Re}\,a_F + i\varepsilon_F\gamma_5\,\mathrm{Im}\,a_F)Fh_2 + \frac{1}{v}\sum_{F=U,D,E}\bar{F}\boldsymbol{M}_{\boldsymbol{F}}(\mathrm{Im}\,a_F - i\varepsilon_F\gamma_5\,\mathrm{Re}\,a_F)Fh_3, \qquad (30)$$

where we have introduced the notation

$$\varepsilon_F \equiv \begin{cases} +1, & \text{for } F = U, \\ -1, & \text{for } F = D, E. \end{cases} \qquad (31)$$

Note that the Yukawa Lagrangian exhibited in Eq. (30) is CP conserving if the alignment parameters a_U, a_D, and a_E are either all real (thereby identifying $h_2 = H$ and $h_3 = A$) or all pure imaginary (where the corresponding CP properties of h_2 and h_3 are reversed).

III. NEUTRAL SCALAR DECAY TO PHOTONS

The diphoton partial decay widths of the neutral scalars are induced at one-loop by diagrams involving W bosons, charged scalars, quarks, and charged leptons. Using the formulas given in Ref. [7],

$$\Gamma(h_k \to \gamma\gamma) = \frac{G_F\alpha^2 m_k^3}{128\pi^3\sqrt{2}}\left\{\left|q_{k1}A_W(\tau_W) + \frac{v^2}{2m_{H^\pm}^2}[q_{k1}Z_3 + \mathrm{Re}(q_{k2}\bar{Z}_7)]A_{H^\pm}(\tau_{H^\pm}) + \sum_f N_{cf}e_f^2[q_{k1} + \mathrm{Re}(q_{k2}^* a_f)]A_f^0(\tau_f)\right|^2 + \left|\sum_f N_{cf}e_f^2\,\mathrm{Im}(q_{k2}^* a_f)A_f^5(\tau_f)\right|^2\right\}, \qquad (32)$$

[5]Flavor-aligned extended Higgs sectors can arise naturally from symmetries of ultraviolet completions of low-energy effective theories of flavor as shown in Refs. [79,81–83]. In such models, departures from exact flavor alignment due to renormalization group running down to the electroweak scale are typically small enough [84,85] to be consistent with all known experimental FCNC bounds.

where the sum over f is taken over three generations of up-type quarks (with $a_f = a_U$), down-type quarks (with $a_f = a_D$), and charged leptons (with $a_f = a_E$), the e_f are the corresponding fermion charges in units of the positron charge e, $N_{cf} = 3$ ($N_{cf} = 1$) for the quarks (leptons), the loop functions A_W, $A_{H^\pm}$, A_f^0 and A_f^5 are listed in Appendix B, and $\tau_X \equiv 4m_X^2/m_k^2$. We cross-checked our results with ScannerS [86], confirming our results for the case $\lambda_6 = \lambda_7 = 0$ in a generic basis of scalar fields, and assuming the Yukawa sector of the type-I 2HDM [87].

Note that for exact Higgs alignment, the partial decay width $\Gamma(h_1 \to \gamma\gamma)$ differs from its SM value by the contribution of the charged Higgs loop that is proportional to $(Z_3)^2$. The contributions of the fermion loops to the diphoton partial decay widths of $h_2 \simeq H$ and $h_3 \simeq A$ vanish in the limit of $a_F = 0$. In this approximation, the diphoton partial decay widths of H and A arise solely from the charged Higgs loop, with contributions proportional to $[\mathrm{Re}\,\bar{Z}_7]^2$ and $[\mathrm{Im}\,\bar{Z}_7]^2$, respectively.

The partial decays widths of the neutral scalars to fermions, WW and ZZ can be obtained by rescaling the one of a hypothetical SM Higgs boson with the same mass [88] by the square of the ratios of the corresponding vertex factors.[6] In this way higher-order QCD and electroweak corrections are included.

IV. ELECTRIC DIPOLE MOMENTS

The most constraining bound on the CP-violating parameters of the general 2HDM derives from the measurement of the electron EDM [27–29],

$$|d_e| \le (1.3 \pm 2.0_{\mathrm{stat}} \pm 0.6_{\mathrm{sys}}) \times 10^{-30}\ e\mathrm{cm}. \tag{33}$$

For calculating the electron EDM within the 2HDM we used the results and the publicly available code provided as supplemental material in Ref. [90] (see Eq. (41) and related discussion in Ref. [90]). As in Sec. III, we again have used ScannerS [86] to cross-check our results for the electron EDM.

The prospects for the neutron EDM ($|d_n|$) and proton EDM ($|d_p|$) are at the level of 10^{-27} $e$cm [29] and 10^{-29} $e$cm [91], respectively. The dominant contributions in the 2HDM arise at the two-loop level via the Barr-Zee diagrams [92] as well as sunset diagrams contributing to the three-gluon Weinberg operator[7] $\tilde{d}_G(m_t)$ [93] (see Fig. 1). The neutron EDM can then be written as [94,95]

$$\begin{aligned} d_n = {} & -(0.20 \pm 0.01) d_u + (0.78 \pm 0.03) d_d \\ & - (0.55 \pm 0.28) e\tilde{d}_u - (1.1 \pm 0.55) e\tilde{d}_d \\ & + (50 \pm 40)\ \mathrm{MeV} e\tilde{d}_G, \end{aligned} \tag{34}$$

where the theory errors associated with the hadronic matrix elements [93,96–101] have been neglected. In Eq. (34), the chromomagnetic contributions have been labeled with a tilde and [102–104]

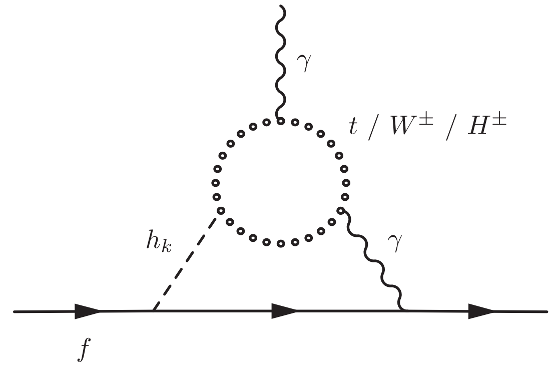

(a)

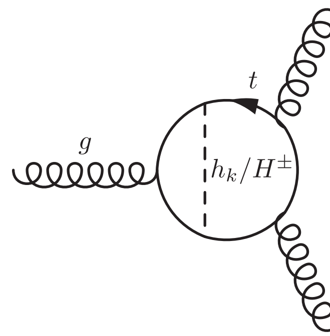

(b)

FIG. 1. Representative Feynman diagrams contributing to EDMs: (a) example of a Barr-Zee diagram that contributes to fermionic EDMs. Note that if a t-quark is in the loop, then a chromomagnetic operator is also induced by replacing both photons with gluons; (b) contribution to the Wilson coefficient of the three-gluon Weinberg operator.

[6]For CP-eigenstates, the Higgs decays widths to light fermion pairs are roughly the same for a CP-even and a CP-odd scalar, whereas the latter has no couplings to gauge bosons [7]. For the case of mixed states, the CP-even and CP-odd scalar couplings to fermions do not interfere when calculating the decay widths and only the CP-even component of a scalar couples to WW and ZZ. Note that complex couplings also lead to the decays $H^\pm \to W^\pm Z$; however with very small branching ratios [89].

[7]There is also another contribution to the three-gluon Weinberg operator at 2-loops, the so-called charged contribution corresponding to the lower Feynman diagram in Fig. 1 with the charged Higgs boson in the propagator inside the loop. However, this contribution is proportional to $\mathrm{Im}(a_D^* a_U)$ and can be safely neglected in our numerical analysis.

TABLE II. Branching ratios of the neutral scalars h_2 and h_3 (with $m_{h_3} = 95$ GeV), for the choice of parameters given by the benchmark point exhibited in Table III with $\mathrm{Im}\,\bar{Z}_7 = 0.4$ and $\mathrm{Re}\,a_U = -0.01$. The branching ratios for the Zh_i mode correspond to $h_2 \to Zh_3$ and $h_3 \to Zh_2$, respectively. Branching ratios less than 10^{-7} are indicated by a zero entry above.

	$b\bar{b}$	$\tau^+\tau^-$	$c\bar{c}$	$\mu^+\mu^-$	W^+W^-	ZZ	gg	$\gamma\gamma$	Zh_1	Zh_i	$W^\pm H^\mp$
$h_2 \simeq H$	0.80	0.084	0.037	2.9×10^{-4}	7.9×10^{-3}	9.0×10^{-4}	0.069	1.5×10^{-3}	0	1.6×10^{-6}	0
$h_3 \simeq A$	0.73	0.076	0.089	2.6×10^{-4}	4.3×10^{-3}	6.1×10^{-4}	0.061	0.037	0	0	0

$$\tilde{d}_G(m_t) = 4g_s^3(m_t)\frac{\sqrt{2}G_F}{(4\pi)^4} \times \sum_{f=t,b}\varepsilon_f[q_{k1} + \mathrm{Re}(q_{k2}^* a_f)]\,\mathrm{Im}(q_{k2}^* a_f)F(m_f, m_k), \tag{35}$$

where $\varepsilon_f = \pm 1$ for $f = t$ (with $a_f = a_U$) and $f = b$ (with $a_f = a_D$) [cf. Eq. (31)], and $F(m, M)$ is defined as

$$F(m_f, m_k) = \frac{m_f^4}{4}\int_0^1 dx \int_0^1 du \frac{u^3 x^3(1-x)}{[m_f^2 x(1-ux) + m_k^2(1-u)(1-x)]^2}. \tag{36}$$

The contributions of light quarks were determined using the prescription described in Eq. (63) of Ref. [90] for recasting the corresponding results of the electron. We used renormalization-group-improved results for the chromomagnetic contribution [102,105]. To obtain the proton EDM, to first approximation one can swap down quarks with up quarks in Eq. (34).

V. PHENOMENOLOGY

As discussed in Sec. IV, $\mathrm{Im}\,\bar{Z}_7$ is the only scalar potential parameter that generates an unsuppressed contribution to the decay width $(h_3 \simeq A) \to \gamma\gamma$. If, in addition, the mixing with other scalars and the flavor-alignment parameters a_F ($F = U$, D, E) are small, then it is possible to enhance the branching ratio, $\mathrm{BR}(h_3 \to \gamma\gamma)$, beyond a value that is accessible in a 2HDM with a $\mathbb{Z}_2$ conserving scalar potential. Let us consider *separately* the diphoton excesses at 95 GeV and 152 GeV as applications for this mechanism.

A. 95 GeV and 98 GeV excesses

Concerning the 95 GeV diphoton excess[8] the combination of ATLAS [35] and CMS [107] data prefers a signal strength for the 95 GeV scalar S of [108]

$$\mu^{\mathrm{LHC}}_{\gamma\gamma,95} = \frac{\sigma^{\mathrm{NP}}(pp \to S_{95} \to \gamma\gamma)}{\sigma^{\mathrm{SM}}(pp \to h_{95} \to \gamma\gamma)} = 0.24^{+0.09}_{-0.08}, \tag{37}$$

where h_{95} represents a (hypothetical) SM-like Higgs boson with a mass of 95 GeV, used to illustrate the (size) of the excess and NP stands for new physics. It has been shown that only small regions in parameter space of the 2HDM with a $\mathbb{Z}_2$ symmetry[9] can explain the 95 GeV excess if this scalar is CP-even [49–52], whereas a CP-odd solution is even more difficult. The LEP collider found a 2.3σ excess for a scalar H in $e^+e^- \to Z^* \to ZH$ [110], which is most pronounced in $H \to b\bar{b}$, resulting [111] in[10]

$$\mu^{\mathrm{LEP}}_{b\bar{b}} = \frac{\sigma^{\mathrm{NP}}(e^+e^- \to ZS_{98})}{\sigma^{\mathrm{SM}}(e^+e^- \to Zh_{98})}\frac{\mathrm{BR}(S_{98} \to b\bar{b})}{\mathrm{BR}(h_{98} \to b\bar{b})} \approx 0.12 \pm 0.06, \tag{38}$$

where the labels are as in Eq. (37).

Here we want to consider the option that the diphoton excess is due to the (mostly) CP-odd scalar $h_3 \simeq A$. While the LEP signal cannot be explained at the same time by h_3, the excess is in fact most pronounced at $\approx$98 GeV, indicating that it could be due to another state, which we shall identify as the mostly CP-even scalar $h_2 \simeq H$. Note that for the sizable mixing angles preferred by LEP ($\theta_{12} \approx 0.3$), h_2 decays dominantly to $b\bar{b}$ with a small branching ratio to photons such that LHC bounds are not relevant, as indicated in Table II. We have two main production mechanisms for h_2 and h_3: Drell-Yan (DY) ($pp \to Z^* \to h_2h_3$, $pp \to W^* \to h_{2,3}H^\pm$) and gluon fusion.[11] In the limit of small mixing angles we have

[8]The ditau excess of CMS [33] at around 100 GeV is not seen by ATLAS [106] and also not confirmed by the b-associated channel of CMS. Therefore, we will disregard the ditau channel here.

[9]The generic 2HDM with a sizable Yukawa coupling of the top quark to $\mathcal{H}_2$ can explain the 95 GeV diphoton excess [109].

[10]We rounded the numbers for the LEP signal strength to one significant digit and adjusted the error to recover the 2.3σ excess reported by LEP.

[11]The gluon-fusion cross section is obtained from rescaling the SM [88], including a factor of $\approx$1.5 due to the axial coupling [112,113]. For the Drell-Yan production cross section, we used MadGraph5_aMC@NLO [114,115], including the next-to-next-to leading log (NNLL) and NLO QCD correction factor of $\approx$1.15 of Refs. [116,117].

TABLE III. Benchmark point used for the interpretation of the $\gamma\gamma$ excesses at 95 GeV and the $b\bar{b}$ excess at 98 GeV. We fixed $a_D = a_E = 0$ and Arg $a_U = -0.03$, and masses are given in units of GeV.

m_{h_1}	m_{h_2}	m_{h_3}	$m_{H^\pm}$	θ_{12}	θ_{13}	Z_2	Z_3	$\mathrm{Re}\,\bar{Z}_7$
125	98	95	130	0.25	0.01	0.2	−0.2	0.1

$$\begin{aligned}
\sigma_{\mathrm{GF}}(pp\to h_3) &\approx \frac{1.5}{1+s_{12}^2}\sigma_{\mathrm{GF}}(pp\to h_{95}) \approx |a_U|^2 100\ \mathrm{pb}\\
\sigma_{\mathrm{DY}}(pp\to h_3H^\pm) &\approx \sigma_{\mathrm{DY}}(pp\to h_2H^\pm) \approx 0.31\ \mathrm{pb}\\
\sigma_{\mathrm{DY}}(pp\to h_3h_2) &\approx 0.28\ \mathrm{pb}
\end{aligned} \tag{39}$$

where we have taken 130 GeV for the charged Higgs mass in light of the ATLAS excess in $t\to(H^\pm\to cb)b$ [118]. For simplicity, let us consider the dependence on a_U and $\mathrm{Im}\,\bar{Z}_7$ while setting $a_D = a_E = 0$, which strongly suppresses an effect in the very constraining electron EDM. We fix the other relevant model parameters as indicated in Table III. The branching ratios of the h_2 and h_3 decay modes corresponding to this benchmark point are exhibited in Table II. In Fig. 2, we show the preferred regions in the $\mathrm{Im}\,\bar{Z}_7 - \mathrm{Re}\,a_U$ plane.[12] Note the complementary between the proton and the neutron EDM. In particular, future EDM measurements can cover most of the parameter space in which the 95 GeV diphoton excess is explained.

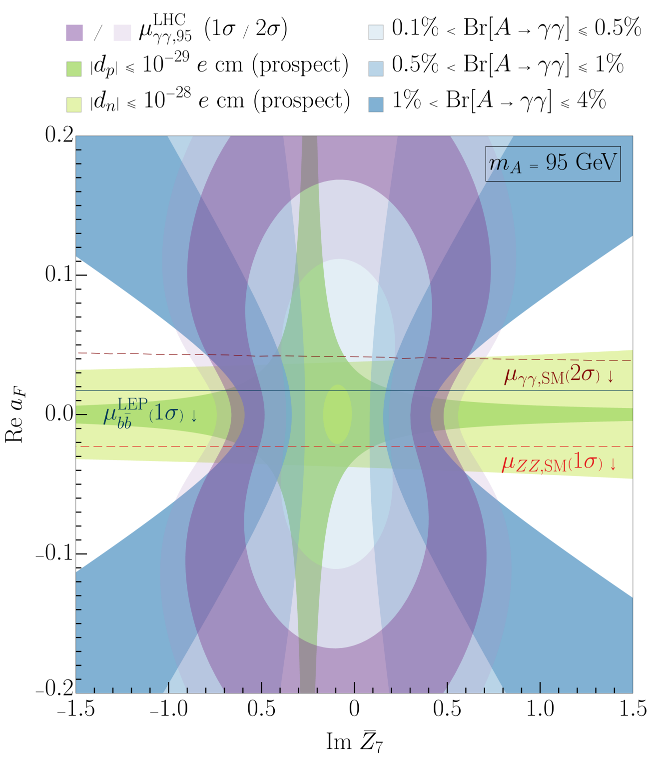

FIG. 2. Preferred regions in the $\mathrm{Im}\,\bar{Z}_7 - \mathrm{Re}\,a_U$ plane from the diphoton excesses at 95 GeV (blue) and the estimated sensitivity of future neutron and proton EDM measurements (green). The regions above the dashed lines are excluded by the SM Higgs signal strength in $h_1\to\gamma\gamma/ZZ$, while the one below the solid line is preferred by the LEP (98 GeV) signal strength. The benchmark point exhibited in Table III fixes the other model parameters.

B. 152 GeV excess

Here, the relevant production process is Drell-Yan as we are considering the associated production of the 152 GeV boson, i.e., $\gamma\gamma + X$ which is significantly more sensitive to physics beyond the SM than the inclusive measurements. From the analysis of Ref. [53],[13] we see that the preference for a nonzero diphoton branching ratio with a best-fit value of $\approx 1.3\%$ is greater than 4σ. Here, we consider for simplicity the case in which the relative coupling strength to all fermions is the same, $a_U = a_D = a_E = a_F$. The branching ratios of the neutral scalars h_2 and h_3 (for $m_{h_3} = 152$ GeV) are given in Table IV for the benchmark point specified in Table V.[14] The comparison of the preferred diphoton branching ratios as well as the bounds from EDMs are shown[15] in Fig. 3. One can see that the electron EDM enforces the product of $\mathrm{Im}\,\bar{Z}_7 \times |a_F|$ to be small, such that the 152 GeV excess can only be explained for small values of the couplings $|a_F|$, corresponding to the region where DY is the main production mechanism. If $a_E = 0$, then the electron EDM constraint would be avoided, but the scenario could still be tested by future neutron and proton EDM measurements. In light of the large branching ratio for $A\to W^\pm H^\mp$ (with, say, the W

[12] Note that charged Higgs boson searches are not constraining for our setup [119] and we checked with HiggsTools [120] that also no other search channels implemented there are violated for this benchmark point. Additionally, for the parameter space explaining the excesses without violating other bounds, we checked for consistency with vacuum stability and perturbative unitarity.

[13] Although Ref. [53] considered the case in which $h_2 \simeq H$ is the 152 GeV candidate, since only branching ratios of $H^\pm$ matter and the branching ratio of the neutral scalar to photons is the fit parameter, the results apply to our case.

[14] In contrast to the benchmark point of Sec. V A where $a_D = 0$, here we have assumed that both a_U and a_D are nonzero. We have checked that values of the charged Higgs mass as low as $m_{H^\pm} = 130$ GeV are not excluded by the observed rate for $b\to s\gamma$, where the dominant new physics contribution (via a charged Higgs loop) is proportional to $\mathrm{Re}(a_D^* a_U)$. Although such low charged Higgs masses are untenable in the Type-II 2HDM [121], the corresponding constraints in the flavor-aligned 2HDM are considerably weaker in a large region of its parameter space [64,122]. In particular, with the benchmark parameters given in Table V, the entire plane shown in Fig. 3 is allowed.

[15] We checked with HiggsTools [120] that the parameter space addressing the observed excesses is consistent with other direct searches, SM Higgs signal strength and electroweak precision data and satisfies vacuum stability and perturbative unitarity.

TABLE IV. Branching ratios of the neutral scalars h_2 and h_3 (with $m_{h_3} = 152$ GeV), for the choice of parameters given by the benchmark point exhibited in Table V with $\mathrm{Im}\,\bar{Z}_7 = 0.8$ and $\mathrm{Re}\,a_F = 0.01$. The branching ratios for the Zh_i mode correspond to $h_2 \to Zh_3$ and $h_3 \to Zh_2$, respectively. Branching ratios less than 10^{-7} are indicated by a zero entry above.

	$b\bar{b}$	$\tau^+\tau^-$	$c\bar{c}$	W^+W^-	ZZ	gg	$\gamma\gamma$	Zh_1	Zh_i	$W^\pm H^\mp$
$h_2 \simeq H$	2.7×10^{-4}	3.3×10^{-5}	1.4×10^{-5}	0.021	7.2×10^{-3}	1.5×10^{-4}	8.5×10^{-7}	4.7×10^{-7}	0.045	0.93
$h_3 \simeq A$	0.026	2.7×10^{-3}	1.6×10^{-3}	1.3×10^{-3}	1.4×10^{-4}	1.3×10^{-4}	0.012	1.0×10^{-4}	0	0.95

TABLE V. Benchmark point used for the interpretation of the $\gamma\gamma + X$ excesses at 152 GeV. We fixed $a_U = a_D = a_E = a_F$ with $\mathrm{Arg}\,a_F = -0.01$, and masses are given in units of GeV.

m_{h_1}	m_{h_2}	m_{h_3}	$m_{H^\pm}$	θ_{12}	θ_{13}	Z_2	Z_3	$\mathrm{Re}\,\bar{Z}_7$
125	200	152	130	0.01	0.001	0.2	−0.2	0.1

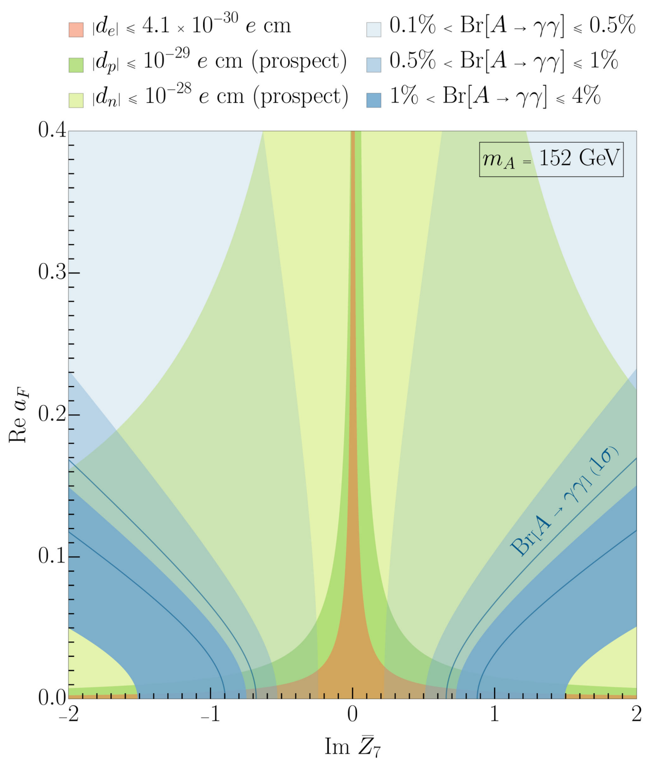

FIG. 3. $\mathrm{BR}(h_3 \to \gamma\gamma)$ in the $\mathrm{Im}\,\bar{Z}_7 - \mathrm{Re}\,a_F$ plane as well as the allowed region from the electron EDM (orange) and the regions where future neutron and proton EDM measurements will be sensitive (green). The preferred 1σ region from the $\gamma\gamma + X$ excesses at 152 GeV is indicated by the band with dark blue solid lines. Constraints from $h_1 \to \gamma\gamma/ZZ$ signal strength are satisfied within the whole depicted area at the 1σ and thus not displayed. The benchmark point exhibited in Table V fixes the other model parameters.

boson off-shell) as shown in Table IV, searches for the charged Higgs boson in future LHC runs will provide an important test of this scenario.

VI. CONCLUSIONS

In this paper, we proposed that a large branching ratio to photons of the (mostly) CP-odd scalar $h_3 \simeq A$ in the flavor-aligned 2HDM can be achieved if the Yukawa flavor-alignment parameters are small and the parameter $\bar{Z}_7$ has a sizable imaginary part. This then acts as a source of CP violation, giving rise to nonvanishing EDMs of fundamental fermions. We considered two benchmark points motivated by the diphoton excesses at 95 GeV and 152 GeV, explored the correlations with the electron EDM, and noted that these regions of parameter space can be tested by future neutron and proton EDM experiments. Moreover, we found that if $h_3 \simeq A$ accounts for the 95 GeV $\gamma\gamma$ excess, then $h_2 \simeq H$ could explain the LEP excess in Higgs-strahlung that is more pronounced at 98 GeV than at 95 GeV.

ACKNOWLEDGMENTS

A. C. thanks Martin Hoferichter for useful discussion on the neutron and proton EDMs. G. C. thanks Wolfgang Altmannshofer for his clarification on the code used in the EDMs calculations. A. C. acknowledges support from a professorship grant from the Swiss National Science Foundation (No. PP00P21_76884). H. E. H. is supported in part by the U.S. Department of Energy Grant No. DE-SC0010107.

APPENDIX A: YUKAWA SECTOR OF THE 2HDM

In the Higgs basis, the 2HDM Yukawa coupling Lagrangian is given by Eq. (27). First, we focus on the terms of the Yukawa Lagrangian involving the neutral scalar fields. It then follows that

$$\begin{aligned}
-\mathcal{L}_Y = {} & (\hat{\boldsymbol{\kappa}}_U)_{mn}\mathcal{H}_1^{0\dagger}\hat{\bar{u}}_{mL}\hat{u}_{nR} + (\hat{\boldsymbol{\rho}}_U)_{mn}\mathcal{H}_2^{0\dagger}\hat{\bar{u}}_{mL}\hat{u}_{nR} \\
& + (\hat{\boldsymbol{\kappa}}_D^\dagger)_{mn}\mathcal{H}_1^{0}\hat{\bar{d}}_{mL}\hat{d}_{nR} + (\hat{\boldsymbol{\rho}}_D^\dagger)_{mn}\mathcal{H}_2^{0}\hat{\bar{d}}_{mL}\hat{d}_{nR} \\
& + (\hat{\boldsymbol{\kappa}}_D^\dagger)_{mn}\mathcal{H}_1^{0}\hat{\bar{e}}_{mL}\hat{e}_{nR} + (\hat{\boldsymbol{\rho}}_E^\dagger)_{mn}\mathcal{H}_2^{0}\hat{\bar{e}}_{mL}\hat{e}_{nR} \\
& + \mathrm{H.c.}
\end{aligned} \tag{A1}$$

where $f_{R,L} \equiv \frac{1}{2}(1 \pm \gamma_5)f$, with $f = u, d, \nu, e$ and there is an implicit sum over the repeated fermion generation indices m, $n \in \{1,2,3\}$. The hatted fields correspond to interaction eigenstates. Setting $\mathcal{H}_1^0 = \mathcal{H}_1^{0\dagger} = v/\sqrt{2}$ yields the fermion mass matrices

$$(\hat{\boldsymbol{M}}_{\boldsymbol{U}})_{mn} = \frac{v}{\sqrt{2}}(\hat{\boldsymbol{\kappa}}_{\boldsymbol{U}})_{mn}, \tag{A2}$$

$$(\hat{\boldsymbol{M}}_{\boldsymbol{D},\boldsymbol{E}})_{mn} = \frac{v}{\sqrt{2}}(\hat{\boldsymbol{\kappa}}^{\dagger}_{\boldsymbol{D},\boldsymbol{E}})_{mn}, \tag{A3}$$

and the neutrino mass matrix $\hat{\boldsymbol{M}}_{\boldsymbol{N}} = 0$. The singular value decompositions of $\hat{\boldsymbol{M}}_U$ and $\hat{\boldsymbol{M}}_D$ yield

$$L_u^{\dagger}\hat{\boldsymbol{M}}_{\boldsymbol{U}}R_u \equiv \boldsymbol{M}_{\boldsymbol{U}}, \qquad L_d^{\dagger}\hat{\boldsymbol{M}}_{\boldsymbol{D}}R_d \equiv \boldsymbol{M}_{\boldsymbol{D}} \tag{A4}$$

where $\boldsymbol{M}_{\boldsymbol{U}}$ and $\boldsymbol{M}_{\boldsymbol{D}}$ are diagonal up- and down-type quark mass matrices with real and nonnegative diagonal elements, and the unitary matrices L_f and R_f ($f = u, d$) relate hatted interaction-eigenstate fermion fields with unhatted mass-eigenstate fields,

$$\hat{f}_{mL} = (L_f)_{mn} f_{nL}, \qquad \hat{f}_{mR} = (R_f)_{mn} f_{nR}. \tag{A5}$$

The Cabibbo-Kobayashi-Maskawa (CKM) matrix is denoted by $\boldsymbol{K} \equiv L_u^{\dagger} L_d$.

Likewise, the singular value decomposition of $\hat{\boldsymbol{M}}_{\boldsymbol{E}}$ yields

$$L_e^{\dagger}\hat{\boldsymbol{M}}_{\boldsymbol{E}}R_e \equiv \boldsymbol{M}_{\boldsymbol{E}}, \tag{A6}$$

where $\boldsymbol{M}_{\boldsymbol{E}}$ is the diagonal charged lepton mass matrix with real and nonnegative diagonal elements, and the mass-eigenstate lepton fields are given (for $f = \nu, e$) by

$$\hat{f}_{mL} = (L_e)_{mn} f_{nL}, \qquad \hat{f}_{mR} = (R_e)_{mn} f_{nR}. \tag{A7}$$

The physical (basis-invariant) ρ-type Yukawa couplings are complex 3×3 matrices,

$$\boldsymbol{\rho}_{\boldsymbol{U}} \equiv L_u^{\dagger}\hat{\boldsymbol{\rho}}_{\boldsymbol{U}}R_u, \qquad \boldsymbol{\rho}^{\dagger}_{\boldsymbol{D}} \equiv L_d^{\dagger}\hat{\boldsymbol{\rho}}^{\dagger}_{\boldsymbol{D}}R_d, \qquad \boldsymbol{\rho}^{\dagger}_{\boldsymbol{E}} \equiv L_e^{\dagger}\hat{\boldsymbol{\rho}}^{\dagger}_{\boldsymbol{E}}R_e, \tag{A8}$$

that generically yield off-diagonal neutral Higgs–fermion interactions. The corresponding neutral Higgs–fermion interactions involving mass-eigenstate scalar and fermion fields can now be obtained. If we additionally include the charged Higgs–fermion interactions starting with Eq. (27) and replace the interaction-eigenstate fields with mass-eigenstate fields, we end up with

$$\begin{aligned}-\mathcal{L}_Y = {}& \bar{U}\left\{\frac{\boldsymbol{M}_{\boldsymbol{U}}}{v}q_{k1} + \frac{1}{\sqrt{2}}[q_{k2}^{*}\boldsymbol{\rho}_{\boldsymbol{U}}\mathcal{P}_R + q_{k2}\boldsymbol{\rho}^{\dagger}_{\boldsymbol{U}}\mathcal{P}_L]\right\}Uh_k + \bar{D}\left\{\frac{\boldsymbol{M}_{\boldsymbol{D}}}{v}q_{k1} + \frac{1}{\sqrt{2}}[q_{k2}\boldsymbol{\rho}^{\dagger}_{\boldsymbol{D}}\mathcal{P}_R + q_{k2}^{*}\boldsymbol{\rho}_{\boldsymbol{D}}\mathcal{P}_L]\right\}Dh_k \\ & + \bar{E}\left\{\frac{\boldsymbol{M}_{\boldsymbol{E}}}{v}q_{k1} + \frac{1}{\sqrt{2}}[q_{k2}\boldsymbol{\rho}^{\dagger}_{\boldsymbol{E}}\mathcal{P}_R + q_{k2}^{*}\boldsymbol{\rho}_{\boldsymbol{E}}\mathcal{P}_L]\right\}Eh_k + \{\bar{U}[\boldsymbol{K}\boldsymbol{\rho}^{\dagger}_{\boldsymbol{D}}\mathcal{P}_R - \boldsymbol{\rho}^{\dagger}_{\boldsymbol{U}}\boldsymbol{K}\mathcal{P}_L]DH^{+} + \bar{N}\boldsymbol{\rho}^{\dagger}_{\boldsymbol{E}}\mathcal{P}_R EH^{+} + \text{H.c.}\},\end{aligned} \tag{A9}$$

with an implicit sum over the index $k = 1,2,3$, where $\mathcal{P}_{R,L} \equiv \frac{1}{2}(1 \pm \gamma_5)$ and the mass-eigenstate fields of the down-type quarks, up-type quarks, charged leptons, and neutrinos are denoted by $D = (d,s,b)^{\mathsf{T}}$, $U \equiv (u,c,t)^{\mathsf{T}}$, $E = (e,\mu,\tau)^{\mathsf{T}}$, and $N = (\nu_e,\nu_\mu,\nu_\tau)^{\mathsf{T}}$, respectively.

As previously noted, the matrices $\boldsymbol{\rho}_{\boldsymbol{F}}$ are in general complex and nondiagonal, which can generate dangerously large tree-level flavor-changing neutral currents (FCNCs) mediated by neutral scalars. In this work, we have employed the flavor-aligned 2HDM [64,74–80] in which the $\boldsymbol{\rho}_{\boldsymbol{F}}$ are proportional to the corresponding diagonal fermion mass matrices $\boldsymbol{M}_{\boldsymbol{F}}$ without imposing any symmetry (such as the $\mathbb{Z}_2$ symmetry used in constructing the type I, II, X, or Y 2HDM [20–22], which naturally yields flavor-diagonal neutral scalar couplings). In particular, we define the *flavor-alignment parameters* a_F via $\hat{\boldsymbol{\rho}}_{\boldsymbol{F}} = a_F\hat{\boldsymbol{\kappa}}_{\boldsymbol{F}}$ for $F = U, D, E$, where the (potentially) complex numbers a_F are invariant under a scalar field basis transformation. In light of Eqs. (A4), (A6), and (A8), it follows that

$$\boldsymbol{\rho}_{\boldsymbol{F}} = \frac{\sqrt{2}}{v}a_F\boldsymbol{M}_{\boldsymbol{F}}, \quad \text{for } F = U, D, E. \tag{A10}$$

Equations (A9) and (A10) then yield the Higgs–fermion Yukawa couplings of the flavor-aligned 2HDM,

$$\begin{aligned}-\mathcal{L}_Y = {}& \frac{1}{v}\bar{U}\boldsymbol{M}_{\boldsymbol{U}}\sum_{k=1}^{3}(q_{k1} + q_{k2}^{*}a_U\mathcal{P}_R + q_{k2}a_U^{*}\mathcal{P}_L)Uh_k + \frac{1}{v}\sum_{F=D,E}\bar{F}\boldsymbol{M}_{\boldsymbol{F}}\sum_{k=1}^{3}(q_{k1} + q_{k2}a_F^{*}\mathcal{P}_R + q_{k2}^{*}a_F\mathcal{P}_L)Fh_k \\ & + \frac{\sqrt{2}}{v}\{\bar{U}[a_D^{*}\boldsymbol{K}\boldsymbol{M}_{\boldsymbol{D}}\mathcal{P}_R - a_U^{*}\boldsymbol{M}_{\boldsymbol{U}}\boldsymbol{K}\mathcal{P}_L]DH^{+} + a_E^{*}\bar{N}\boldsymbol{M}_{\boldsymbol{E}}\mathcal{P}_R EH^{+} + \text{H.c.}\}.\end{aligned} \tag{A11}$$

APPENDIX B: LOOP FUNCTIONS

We list the loop functions used in the computations of the partial decay widths of the scalars to two photons [7]

$$A_W(\tau) = 2 + 3\tau + 3\tau(2 - \tau)g(\tau) \tag{B1}$$

$$A_{H^\pm}(\tau) = \tau[1 - \tau g(\tau)] \tag{B2}$$

$$A_f^0(\tau) = -2\tau[1 + (1 - \tau)g(\tau)] \tag{B3}$$

$$A_f^5(\tau) = -2\tau g(\tau) \tag{B4}$$

where the function $g(\tau)$ is given by

$$g(\tau) = \begin{cases} \left[\sin^{-1}\left(\sqrt{1/\tau}\right)\right]^2, & \text{for } \tau \geq 1, \\ -\frac{1}{4}\left[\log\left(\frac{1+\sqrt{1-\tau}}{1-\sqrt{1-\tau}}\right) - i\pi\right]^2, & \text{for } \tau < 1. \end{cases} \tag{B5}$$

[1] G. Aad *et al.* (ATLAS Collaboration), Observation of a new particle in the search for the Standard Model Higgs boson with the ATLAS detector at the LHC, Phys. Lett. B **716**, 1 (2012).

[2] S. Chatrchyan *et al.* (CMS Collaboration), Observation of a new boson at a mass of 125 GeV with the CMS experiment at the LHC, Phys. Lett. B **716**, 30 (2012).

[3] A. Crivellin and B. Mellado, Anomalies in particle physics and their implications for physics beyond the standard model, Nat. Rev. Phys. **6**, 294 (2024).

[4] T. D. Lee, A theory of spontaneous *T* violation, Phys. Rev. D **8**, 1226 (1973).

[5] S. Weinberg, Gauge theory of *CP* violation, Phys. Rev. Lett. **37**, 657 (1976).

[6] H. Georgi and M. Machacek, Doubly charged Higgs bosons, Nucl. Phys. **B262**, 463 (1985).

[7] J. F. Gunion, H. E. Haber, G. Kane, and S. Dawson, *The Higgs Hunter's Guide* (Westview Press, Boulder, CO, 2000).

[8] Y. Grossman, Phenomenology of models with more than two Higgs doublets, Nucl. Phys. **B426**, 355 (1994).

[9] R. A. Porto and A. Zee, The private Higgs, Phys. Lett. B **666**, 491 (2008).

[10] I. P. Ivanov, Building and testing models with extended Higgs sectors, Prog. Part. Nucl. Phys. **95**, 160 (2017).

[11] G. White, *Electroweak Baryogenesis (Second Edition): An introduction* (IOP Publishing, Bristol, UK, 2022), 10.1088/978-0-7503-3571-3.

[12] G. C. Branco, P. M. Ferreira, L. Lavoura, M. N. Rebelo, M. Sher, and J. P. Silva, Theory and phenomenology of two-Higgs-doublet models, Phys. Rep. **516**, 1 (2012).

[13] A. D. Sakharov, Violation of *CP* Invariance, *C* asymmetry, and baryon asymmetry of the Universe, Pis'ma Zh. Eksp. Teor. Fiz. **5**, 32 (1967).

[14] A. G. Cohen, D. B. Kaplan, and A. E. Nelson, Progress in electroweak baryogenesis, Annu. Rev. Nucl. Part. Sci. **43**, 27 (1993).

[15] M. Trodden, Electroweak baryogenesis: A Brief review, in *Proceedings of the 33rd Rencontres de Moriond: Electroweak Interactions and Unified Theories* (1998), pp. 471–480; arXiv:hep-ph/9805252.

[16] A. Riotto and M. Trodden, Recent progress in baryogenesis, Annu. Rev. Nucl. Part. Sci. **49**, 35 (1999).

[17] D. E. Morrissey and M. J. Ramsey-Musolf, Electroweak baryogenesis, New J. Phys. **14**, 125003 (2012).

[18] P. Fileviez Perez *et al.*, On baryon and lepton number violation, arXiv:2208.00010.

[19] C. E. M. Wagner, Electroweak baryogenesis and Higgs physics, Lett. High Energy Phys. **2023**, 466 (2023).

[20] L. J. Hall and M. B. Wise, Flavor changing Higgs boson couplings, Nucl. Phys. **B187**, 397 (1981).

[21] V. D. Barger, J. L. Hewett, and R. J. N. Phillips, New constraints on the charged Higgs sector in two Higgs doublet models, Phys. Rev. D **41**, 3421 (1990).

[22] M. Aoki, S. Kanemura, K. Tsumura, and K. Yagyu, Models of Yukawa interaction in the two Higgs doublet model, and their collider phenomenology, Phys. Rev. D **80**, 015017 (2009).

[23] P. Basler, L. Biermann, M. Mühlleitner, and J. Müller, Electroweak baryogenesis in the *CP*-violating two-Higgs doublet model, Eur. Phys. J. C **83**, 57 (2023).

[24] M. Pospelov and A. Ritz, CKM benchmarks for electron electric dipole moment experiments, Phys. Rev. D **89**, 056006 (2014).

[25] Y. Yamaguchi and N. Yamanaka, Large long-distance contributions to the electric dipole moments of charged leptons in the Standard Model, Phys. Rev. Lett. **125**, 241802 (2020).

[26] Y. Yamaguchi and N. Yamanaka, Quark level and hadronic contributions to the electric dipole moment of charged leptons in the Standard Model, Phys. Rev. D **103**, 013001 (2021).

[27] T. S. Roussy *et al.*, An improved bound on the electron's electric dipole moment, Science **381**, adg4084 (2023).

[28] C. Abel *et al.*, Measurement of the permanent electric dipole moment of the neutron, Phys. Rev. Lett. **124**, 081803 (2020).

[29] T. Higuchi (on behalf of the TUCAN collaboration), Prospects for a neutron EDM measurement with an advanced ultracold neutron source at TRIUMF, EPJ Web Conf. **262**, 01015 (2022).

[30] G. Aad *et al.* (ATLAS Collaboration), A detailed map of Higgs boson interactions by the ATLAS experiment ten

years after the discovery, Nature (London) **607**, 52 (2022); **612**, E24 (2022); **623**, E5 (2023).
[31] A. Tumasyan *et al.* (CMS Collaboration), A portrait of the Higgs boson by the CMS experiment ten years after the discovery, Nature (London) **607**, 60 (2022); **623**, E4 (2023).
[32] A. M. Sirunyan *et al.* (CMS Collaboration), Search for a Standard Model-like Higgs boson in the mass range between 70 and 110 GeV in the diphoton final state in proton-proton collisions at $\sqrt{s} = 8$ and 13 TeV, Phys. Lett. B **793**, 320 (2019).
[33] A. Tumasyan *et al.* (CMS Collaboration), Searches for additional Higgs bosons and for vector leptoquarks in $\tau\tau$ final states in proton-proton collisions at $\sqrt{s} = 13$ TeV, J. High Energy Phys. 07 (2023) 073.
[34] A. Tumasyan *et al.* (CMS Collaboration), Search for a new resonance decaying into two spin-0 bosons in a final state with two photons and two bottom quarks in proton-proton collisions at $\sqrt{s} = 13$ TeV, J. High Energy Phys. 05 (2024) 316.
[35] G. Aad *et al.* (ATLAS Collaboration), Search for diphoton resonances in the 66 to 110 GeV mass range using pp collisions at $\sqrt{s} = 13$ TeV with the ATLAS detector, J. High Energy Phys. 01 (2025) 053.
[36] G. Aad *et al.* (ATLAS Collaboration), Search for dark matter in events with missing transverse momentum and a Higgs boson decaying into two photons in pp collisions at $\sqrt{s} = 13$ TeV with the ATLAS detector, J. High Energy Phys. 10 (2021) 013.
[37] G. Aad *et al.* (ATLAS Collaboration), Model-independent search for the presence of new physics in events including $H \to \gamma\gamma$ with $\sqrt{s} = 13$ TeV pp data recorded by the ATLAS detector at the LHC, J. High Energy Phys. 07 (2023) 176.
[38] G. Aad *et al.* (ATLAS Collaboration), Search for non-resonant Higgs boson pair production in final states with leptons, taus, and photons in pp collisions at $\sqrt{s} = 13$ TeV with the ATLAS detector, J. High Energy Phys. 08 (2024) 164.
[39] A. Crivellin, Y. Fang, O. Fischer, S. Bhattacharya, M. Kumar, E. Malwa, B. Mellado, N. Rapheeha, X. Ruan, and Q. Sha, Accumulating evidence for the associated production of a new Higgs boson at the LHC, Phys. Rev. D **108**, 115031 (2023).
[40] S. Bhattacharya, G. Coloretti, A. Crivellin, S.-E. Dahbi, Y. Fang, M. Kumar, and B. Mellado, Growing excesses of new scalars at the electroweak scale, arXiv:2306.17209.
[41] G. Coloretti, A. Crivellin, and B. Mellado, Combined explanation of LHC multilepton, diphoton, and top-quark excesses, Phys. Rev. D **110**, 073001 (2024).
[42] S. Ashanujjaman, S. Banik, G. Coloretti, A. Crivellin, S. P. Maharathy, and B. Mellado, Explaining the $\gamma\gamma + X$ excesses at $\approx$151.5 GeV via the Drell-Yan production of a Higgs triplet, Phys. Lett. B **862**, 139298 (2025).
[43] A. Crivellin, S. Ashanujjaman, S. Banik, G. Coloretti, S. P. Maharathy, and B. Mellado, Growing evidence for a Higgs triplet, arXiv:2404.14492.
[44] B. Fuks, M. D. Goodsell, and T. Murphy, Monojets from compressed weak frustrated dark matter, Phys. Rev. D **111**, 055010 (2025).
[45] O. Fischer *et al.*, Unveiling hidden physics at the LHC, Eur. Phys. J. C **82**, 665 (2022).
[46] S. von Buddenbrock, N. Chakrabarty, A. S. Cornell, D. Kar, M. Kumar, T. Mandal, B. Mellado, B. Mukhopadhyaya, R. G. Reed, and X. Ruan, Phenomenological signatures of additional scalar bosons at the LHC, Eur. Phys. J. C **76**, 580 (2016).
[47] G. Coloretti, A. Crivellin, S. Bhattacharya, and B. Mellado, Searching for low-mass resonances decaying into W bosons, Phys. Rev. D **108**, 035026 (2023).
[48] S. Banik, G. Coloretti, A. Crivellin, and B. Mellado, Uncovering new Higgses in the LHC analyses of differential $t\bar{t}$ cross sections, J. High Energy Phys. 01 (2025) 155.
[49] U. Haisch and A. Malinauskas, Let there be light from a second light Higgs doublet, J. High Energy Phys. 03 (2018) 135.
[50] D. Azevedo, T. Biekötter, and P. M. Ferreira, 2HDM interpretations of the CMS diphoton excess at 95 GeV, J. High Energy Phys. 11 (2023) 017.
[51] R. Benbrik, M. Boukidi, S. Moretti, and S. Semlali, Explaining the 96 GeV Di-photon anomaly in a generic 2HDM Type-III, Phys. Lett. B **832**, 137245 (2022).
[52] R. Benbrik, M. Boukidi, and S. Moretti, Superposition of CP-even and CP-odd Higgs resonances: Explaining the 95 GeV excesses within a two-Higgs doublet model, Phys. Rev. D **110**, 115030 (2024).
[53] S. Banik and A. Crivellin, Explanation of the excesses in associated di-photon production at 152 GeV in 2HDM, J. High Energy Phys. 10 (2024) 203.
[54] S. Davidson and H. E. Haber, Basis-independent methods for the two-Higgs-doublet model, Phys. Rev. D **72**, 035004 (2005); **72**, 099902(E) (2005).
[55] H. E. Haber and D. O'Neil, Basis-independent methods for the two-Higgs-doublet model. II. The significance of $\tan\beta$, Phys. Rev. D **74**, 015018 (2006); **74**, 059905(E) (2006).
[56] H. E. Haber and D. O'Neil, Basis-independent methods for the two-Higgs-doublet model III: The CP-conserving limit, custodial symmetry, and the oblique parameters S, T, U, Phys. Rev. D **83**, 055017 (2011).
[57] R. Boto, T. V. Fernandes, H. E. Haber, J. C. Romão, and J. P. Silva, Basis-independent treatment of the complex 2HDM, Phys. Rev. D **101**, 055023 (2020).
[58] H. Georgi and D. V. Nanopoulos, Suppression of flavor changing effects from neutral spinless meson exchange in gauge theories, Phys. Lett. **82B**, 95 (1979).
[59] L. Lavoura, Signatures of discrete symmetries in the scalar sector, Phys. Rev. D **50**, 7089 (1994).
[60] L. Lavoura and J. P. Silva, Fundamental CP violating quantities in a $\mathrm{SU}(2) \times \mathrm{U}(1)$ model with many Higgs doublets, Phys. Rev. D **50**, 4619 (1994).
[61] F. J. Botella and J. P. Silva, Jarlskog-like invariants for theories with scalars and fermions, Phys. Rev. D **51**, 3870 (1995).
[62] G. C. Branco, L. Lavoura, and J. P. Silva, *CP Violation* (Oxford University Press, Oxford, UK, 1999).
[63] H. E. Haber, V. Keus, and R. Santos, P-even, CP-violating signals in scalar-mediated processes, Phys. Rev. D **106**, 095038 (2022).
[64] J. M. Connell, P. Ferreira, and H. E. Haber, Accommodating hints of new heavy scalars in the framework of the

flavor-aligned two-Higgs-doublet model, Phys. Rev. D **108**, 055031 (2023).
[65] I. F. Ginzburg, M. Krawczyk, and P. Osland, Potential of photon collider in resolving SM like scenarios, Nucl. Instrum. Methods Phys. Res., Sect. A **472**, 149 (2001).
[66] J. F. Gunion and H. E. Haber, The *CP* conserving two Higgs doublet model: The approach to the decoupling limit, Phys. Rev. D **67**, 075019 (2003).
[67] N. Craig, J. Galloway, and S. Thomas, Searching for signs of the second Higgs doublet, arXiv:1305.2424.
[68] D. M. Asner *et al.*, ILC Higgs white paper, in *Proceedings of the Community Summer Study 2013: Snowmass on the Mississippi* (2013); arXiv:1310.0763.
[69] M. Carena, I. Low, N. R. Shah, and C. E. M. Wagner, Impersonating the standard model Higgs boson: Alignment without decoupling, J. High Energy Phys. 04 (2014) 015.
[70] H. E. Haber, The Higgs data and the decoupling limit, in *Proceedings of the 1st Toyama International Workshop on Higgs as a Probe of New Physics* (2013); arXiv:1401.0152.
[71] S. L. Glashow and S. Weinberg, Natural conservation laws for neutral currents, Phys. Rev. D **15**, 1958 (1977).
[72] E. A. Paschos, Diagonal neutral currents, Phys. Rev. D **15**, 1966 (1977).
[73] A. Crivellin, A. Kokulu, and C. Greub, Flavor-phenomenology of two-Higgs-doublet models with generic Yukawa structure, Phys. Rev. D **87**, 094031 (2013).
[74] A. Pich and P. Tuzon, Yukawa alignment in the two-Higgs-doublet model, Phys. Rev. D **80**, 091702 (2009).
[75] A. Pich, Flavour constraints on multi-Higgs-doublet models: Yukawa alignment, Nucl. Phys. B, Proc. Suppl. **209**, 182 (2010).
[76] O. Eberhardt, A. P. Martínez, and A. Pich, Global fits in the aligned two-Higgs-doublet model, J. High Energy Phys. 05 (2021) 005.
[77] S. Y. Choi, J. S. Lee, and J. Park, Alignment of Yukawa couplings in two Higgs doublet models, arXiv:2011.04978.
[78] J. S. Lee and J. Park, Yukawa alignment revisited in the Higgs basis, Phys. Rev. D **106**, 015023 (2022).
[79] H. Serodio, Yukawa alignment in a multi Higgs doublet model: An effective approach, Phys. Lett. B **700**, 133 (2011).
[80] G. Cree and H. E. Logan, Yukawa alignment from natural flavor conservation, Phys. Rev. D **84**, 055021 (2011).
[81] S. Knapen and D. J. Robinson, Disentangling mass and mixing hierarchies, Phys. Rev. Lett. **115**, 161803 (2015).
[82] D. Egana-Ugrinovic, S. Homiller, and P. Meade, Aligned and spontaneous flavor violation, Phys. Rev. Lett. **123**, 031802 (2019).
[83] D. Egana-Ugrinovic, S. Homiller, and P. R. Meade, Higgs bosons with large couplings to light quarks, Phys. Rev. D **100**, 115041 (2019).
[84] C. B. Braeuninger, A. Ibarra, and C. Simonetto, Radiatively induced flavour violation in the general two-Higgs doublet model with Yukawa alignment, Phys. Lett. B **692**, 189 (2010).
[85] S. Gori, H. E. Haber, and E. Santos, High scale flavor alignment in two-Higgs doublet models and its phenomenology, J. High Energy Phys. 06 (2017) 110.
[86] M. Mühlleitner, M. O. P. Sampaio, R. Santos, and J. Wittbrodt, `ScannerS`: Parameter scans in extended scalar sectors, Eur. Phys. J. C **82**, 198 (2022).
[87] D. Fontes, M. Mühlleitner, J. C. Romão, R. Santos, J. P. Silva, and J. Wittbrodt, The C2HDM revisited, J. High Energy Phys. 02 (2018) 073.
[88] D. de Florian *et al.* (LHC Higgs Cross Section Working Group Collaboration), Handbook of LHC Higgs cross sections: 4. Deciphering the nature of the Higgs sector, arXiv:1610.07922.
[89] S. Kanemura and Y. Mura, Loop induced $H^\pm W^\mp Z$ vertices in the general two Higgs doublet model with *CP* violation, J. High Energy Phys. 10 (2024) 041.
[90] W. Altmannshofer, S. Gori, N. Hamer, and H. H. Patel, Electron EDM in the complex two-Higgs doublet model, Phys. Rev. D **102**, 115042 (2020).
[91] Z. Omarov, H. Davoudiasl, S. Haciomeroglu, V. Lebedev, W. M. Morse, Y. K. Semertzidis, A. J. Silenko, E. J. Stephenson, and R. Suleiman, Comprehensive symmetric-hybrid ring design for a proton EDM experiment at below 10^{-29} $e \cdot$cm, Phys. Rev. D **105**, 032001 (2022).
[92] S. M. Barr and A. Zee, Electric dipole moment of the electron and of the neutron, Phys. Rev. Lett. **65**, 21 (1990); **65**, 2920 (1990).
[93] S. Weinberg, Larger Higgs exchange terms in the neutron electric dipole moment, Phys. Rev. Lett. **63**, 2333 (1989).
[94] R. Alarcon *et al.*, Electric dipole moments and the search for new physics, in *Proceedings of the The Particle Physics Community Planning Exercise (Snowmass 2021)*; arXiv:2203.08103.
[95] T. Bhattacharya, V. Cirigliano, R. Gupta, E. Mereghetti, and B. Yoon, Contribution of the QCD Θ-term to the nucleon electric dipole moment, Phys. Rev. D **103**, 114507 (2021).
[96] N. Yamanaka and E. Hiyama, Weinberg operator contribution to the nucleon electric dipole moment in the quark model, Phys. Rev. D **103**, 035023 (2021).
[97] J. Dragos, T. Luu, A. Shindler, J. de Vries, and A. Yousif, Confirming the existence of the strong *CP* problem in lattice QCD with the gradient flow, Phys. Rev. C **103**, 015202 (2021).
[98] R. Gupta, B. Yoon, T. Bhattacharya, V. Cirigliano, Y.-C. Jang, and H.-W. Lin, Flavor diagonal tensor charges of the nucleon from $(2+1+1)$-flavor lattice QCD, Phys. Rev. D **98**, 091501 (2018).
[99] T. Bhattacharya, V. Cirigliano, R. Gupta, H.-W. Lin, and B. Yoon, Neutron electric dipole moment and tensor charges from lattice QCD, Phys. Rev. Lett. **115**, 212002 (2015).
[100] M. Pospelov and A. Ritz, Neutron EDM from electric and chromoelectric dipole moments of quarks, Phys. Rev. D **63**, 073015 (2001).
[101] J. Hisano, J. Y. Lee, N. Nagata, and Y. Shimizu, Reevaluation of neutron electric dipole moment with QCD sum rules, Phys. Rev. D **85**, 114044 (2012).
[102] M. Jung and A. Pich, Electric dipole moments in two-Higgs-doublet Models, J. High Energy Phys. 04 (2014) 076.

[103] S. Teunissen, Lepton and neutron EDM as probe of general two Higgs doublet model, Proc. Sci. EPS- HEP2023 (**2024**) 469 [arXiv:2311.05184].

[104] W. Kuramoto, Light stop, heavy Higgs, and heavy gluino in supersymmetric standard models with extra matters, Proc. Sci. KMI2017 (**2017**) 039.

[105] W. Dekens, J. de Vries, M. Jung, and K. K. Vos, The phenomenology of electric dipole moments in models of scalar leptoquarks, J. High Energy Phys. 01 (2019) 069.

[106] G. Aad *et al.* (ATLAS Collaboration), Measurements of Higgs boson production cross-sections in the $H \to \tau^+\tau^-$ decay channel in pp collisions at $\sqrt{s} = 13$ TeV with the ATLAS detector, J. High Energy Phys. 08 (2022) 175.

[107] A. Hayrapetyan *et al.* (CMS Collaboration), Search for a Standard Model-like Higgs boson in the mass range between 70 and 110 GeV in the diphoton final state in proton-proton collisions at $\sqrt{s} = 13$ TeV, Phys. Lett. B **860**, 139067 (2025).

[108] T. Biekötter, S. Heinemeyer, and G. Weiglein, 95.4 GeV diphoton excess at ATLAS and CMS, Phys. Rev. D **109**, 035005 (2024).

[109] A. Crivellin, J. Heeck, and D. Müller, Large $h \to bs$ in generic two-Higgs-doublet models, Phys. Rev. D **97**, 035008 (2018).

[110] R. Barate *et al.* (LEP Working Group for Higgs boson searches, ALEPH, DELPHI, L3, and OPAL Collaborations), Search for the Standard Model Higgs boson at LEP, Phys. Lett. B **565**, 61 (2003).

[111] J. Cao, X. Guo, Y. He, P. Wu, and Y. Zhang, Diphoton signal of the light Higgs boson in natural NMSSM, Phys. Rev. D **95**, 116001 (2017).

[112] S. Dawson, S. Dittmaier, and M. Spira, Neutral Higgs boson pair production at hadron colliders: QCD corrections, Phys. Rev. D **58**, 115012 (1998).

[113] M. Spira, Higgs boson production and decay at hadron colliders, Prog. Part. Nucl. Phys. **95**, 98 (2017).

[114] J. Alwall, M. Herquet, F. Maltoni, O. Mattelaer, and T. Stelzer, MadGraph5: Going beyond, J. High Energy Phys. 06 (2011) 128.

[115] J. Alwall *et al.*, The automated computation of tree-level and next-to-leading order differential cross sections, and their matching to parton shower simulations, J. High Energy Phys. 07 (2014) 079.

[116] R. Ruiz, QCD corrections to pair production of type III seesaw leptons at hadron colliders, J. High Energy Phys. 12 (2015) 165.

[117] A. H. Ajjath, B. Fuks, H.-S. Shao, and Y. Simon, Precision predictions for exotic lepton production at the large hadron collider, Phys. Rev. D **107**, 075011 (2023).

[118] G. Aad *et al.* (ATLAS Collaboration), Search for a light charged Higgs boson in $t \to H^\pm b$ decays, with $H^\pm \to cb$, in the lepton + jets final state in proton-proton collisions at $\sqrt{s} = 13$ TeV with the ATLAS detector, J. High Energy Phys. 09 (2023) 004.

[119] G. Aad *et al.* (ATLAS Collaboration), Search for a light charged Higgs boson in $t \to H^\pm b$ decays, with $H^\pm \to cs$, in pp collisions at $\sqrt{s} = 13$ TeV with the ATLAS detector, Eur. Phys. J. C **85**, 153 (2025).

[120] H. Bahl, T. Biekötter, S. Heinemeyer, C. Li, S. Paasch, G. Weiglein, and J. Wittbrodt, HiggsTools: BSM scalar phenomenology with new versions of HiggsBounds and HiggsSignals, Comput. Phys. Commun. **291**, 108803 (2023).

[121] M. Misiak, A. Rehman, and M. Steinhauser, Towards $\bar{B} \to X_s\gamma$ at the NNLO in QCD without interpolation in m$_c$, J. High Energy Phys. 06 (2020) 175.

[122] A. M. Coutinho, A. Karan, V. Miralles, and A. Pich, Light scalars within the $\mathcal{CP}$-conserving aligned-two-Higgs-doublet model, J. High Energy Phys. 02 (2025) 057.